

Role of momentum in the generator-coordinate method applied to barrier penetration

K. Hagino¹ and G.F. Bertsch²

¹ *Department of Physics, Kyoto University, Kyoto 606-8502, Japan*

² *Department of Physics and Institute for Nuclear Theory, Box 351560, University of Washington, Seattle, Washington 98915, USA*

Nuclear fission at barrier-top energies is conventionally modeled by a one-dimensional Schrödinger equation applied to internal fission channels, but that treatment is hard to justify in the configuration-interaction approach to nuclear Hamiltonians. Here we show that inclusion of states of finite momentum by the Generator Coordinate Method (GCM) considerably extends the range of energies at which GCM-based Hamiltonians could reproduce the Schrödinger treatment. The transmission probabilities for crossing the barrier are calculated by a discrete version of Kohn's variational method, which may also be useful for other systems of interacting fermions.

I. INTRODUCTION

As discussed in our previous papers in this series[1, 2], there are many unanswered questions about the dynamics of nuclear fission that require a fully microscopic theory to answer definitively. Most fundamentally, should one treat the dynamics as largely diffusive as in Kramer's model [3], or as motion along a collective coordinate as in Bohr and Wheeler's original transition-state model [4]? Given the success of the configuration-interaction (CI) framework for calculating energies and spectroscopic properties, that approach should be explored for fission theory as well. Our previous papers have advocated using the CI framework and particularly the Generator Coordinate Method (GCM) to build a reaction theory of fission that might possibly address the questions. The generator-coordinate method (GCM) has been a very useful tool for constructing many-particle wave functions, particularly as applied to deformed systems undergoing shape changes; see Ref. [5] for an early study.

Absent a microscopic theory, barrier traversal has been treated by one-dimensional Schrödinger dynamics since the pioneering work of Hill and Wheeler [6], and continuing up to the present era [7–10]. Since that approach is so well established, one can ask what is required for the discrete-basis CI Hamiltonian to reproduce the Schrödinger results. In our previous work, we showed how a Hamiltonian constructed from a chain of GCM states could produce the transmission probabilities in a limited range of energies, requiring barrier heights no higher than a few (2-3) times larger than the zero-point energies of the states. Here we show that adding a second state on each site of the chain can double the useful energy range. That is more than enough to reproduce the transmission probabilities calculated in the Schrödinger approach.

This article is organized as follows. We first summarize the construction of a simplified Hamiltonian compatible with the GCM framework. Next we extend the space to include higher momentum states and assess their fidelity as momentum eigenstates. Then we formulate a computationally tractable reaction theory following Kohn's [11] employment of asymptotic channel wave functions.

Transmission probabilities calculated in that scheme are reported in Sec. IV and compared with the Schrödinger results.

II. THE DISCRETE-BASIS HAMILTONIAN

The target Schrödinger Hamiltonian has the usual form

$$H = -\frac{\hbar^2}{2M} \frac{\partial^2}{\partial x^2} + V(x), \quad (1)$$

where x is a collective coordinate defined by the GCM constraints. The M in the kinetic term is the collective inertia associated with the coordinate and $V(x)$ is the barrier potential. To mimic a discrete-basis GCM Hamiltonian basis, we assume that the wave function can be factorized into a Gaussian wave packet along the collective coordinate times an internal wave function that need not be specified. The space consists of a mesh of these wave packets centered on equally spaced points Δx along the collective coordinate. The model is completely determined by the Hamiltonian and overlap matrix elements between these states, $H_{ij} = \langle i|H|j \rangle$ and $N_{ij} = \langle i|j \rangle$. We assume these elements depend only on the separation between the two states i and j along the chain, apart from the barrier potential V . The Gaussian wave packet is parameterized as the ground-state harmonic oscillator wave function

$$\phi_{0,x_i}(x) = \frac{1}{\pi^{1/4} s^{1/2}} e^{-(x-x_i)^2/2s^2}. \quad (2)$$

Here the subscript x_i denotes the center point of the collective coordinate in the GCM wave packet. With the above definition the overlap matrix elements are

$$N_{i,j} = e^{-(i-j)^2 \Delta x^2 / 4s^2}. \quad (3)$$

The Hamiltonian matrix elements are parameterized in the well-known Gaussian overlap approximation (GOA) as [12]

$$H_{i,j} = N_{i,j} E_q (1 - (i-j)^2 \Delta x^2 / s^2). \quad (4)$$

Here

$$E_q = \frac{\hbar^2}{4M s^2} \quad (5)$$

is the zero-point kinetic energy in the collective coordinate. Of course in an actual GCM Hamiltonian the matrix elements will not be so regular as assumed in Eqs. (3,4).

Note that the parameter Δx is purely numerical and must be chosen with some care. If it is too small the diagonalization of the matrix Hamiltonian equation

$$\mathbf{H}\psi = E\mathbf{N}\psi \quad (6)$$

becomes numerically unstable. On the other hand, if it is too large the space of configurations along the collective path is not well sampled. We choose the parameter value $\Delta x = 5^{1/2}s$ as a somewhat arbitrary compromise between these considerations [13].

The new ingredient in this work is the explicit introduction of momentum in the wave function at each site. This can be done in different ways, depending on how the configurations are constructed [14, 15]. In the GCM framework one could add a momentum constraint or simply take derivatives with respect to x_i , the central position of the wave packet at site i . The resulting wave packet is just the first excited harmonic oscillator wave function,

$$\phi_{1,x_i}(x) = 2^{1/2}(x - x_i)e^{-(x-x_i)^2/2s^2}/\pi^{1/4}. \quad (7)$$

Our space of states will be defined with ϕ_{1,x_1} as the second state on the site.

III. CONSTRUCTION OF PLANE WAVES AND THEIR PROPERTIES

Wave functions simulating plane waves are trivial to construct for states with a fixed internal structure on equally spaced grid points; the amplitudes on adjacent sites are related by identical phase factors $e^{i\theta}$. It is less obvious how to build them when there are two or more states at each grid point. In this work we determine them from eigensolutions of the kinetic Hamiltonian as follows. In the first step, a periodic matrix Hamiltonian is defined on a ring of N_q mesh points. Translational symmetry is imposed by requiring H and N to depend only on the difference between the site variables, that is

$$\langle \mu, x_i | H | \mu', x_j \rangle = H_{|i-j|, \mu, \mu'} \quad (8)$$

Here μ labels the states on a site. The dimension of the space is thus $N_q N_s$ where N_s is the number of states on each site. The overlap matrix is constructed in the same way. The matrices are band-diagonal with nonzero matrix elements extending to N_{od} sites on either side of the diagonal. For our numerical study we include next-to-nearest neighbor interactions, $N_{\text{od}} = 2$. Details of the matrix elements are given in the Appendix A.

Next one solves the generalized eigenvalue equation Eq. (6) expressing the eigenstates in terms of amplitudes \vec{f}_0 and \vec{f}_1 :

$$\psi = \sum_i (f_{0,i} \phi_{0,x_i} + f_{1,i} \phi_{1,x_i}). \quad (9)$$

All the eigenvalues and amplitudes f are real, and all but two of them have a partner with the same eigenvalue. In fact, these eigenvectors and energies can be calculated much more simply from the formulas derived in Appendix B.

The traveling waves are constructed from paired eigenvectors ψ_1, ψ_2 as

$$\psi_k = \psi_1 + i\psi_2 \quad (10)$$

$$\psi_{-k} = \psi_1 - i\psi_2. \quad (11)$$

The subscript $\pm k$ denotes the momentum of the state, which is still to be determined. Within each of these traveling waves the amplitudes at adjacent sites are related by $e^{\pm i\theta}$. Due to the ring structure of the Hamiltonian the phase θ is quantized with the form

$$\theta = \pm m \frac{\pi}{sN_q}. \quad (12)$$

where the m can be restricted to the range $-N_q < m < N_q$. For Hamiltonians with a single state on site, the states approximate eigenstates of the momentum operator with $k \approx \theta/\Delta x$. In the Hamiltonian with an added momentum state on the sites the number of eigenstates is doubled. The lower energy states become more accurate approximations to the same momenta in the range $0 < |k| < \pi/\Delta x$. However, the phase change for the higher energy states is better interpreted by the assignment $k \approx (\theta + \pi)\Delta x$. The situation is depicted in Fig. 1. The momentum assignments based solely on the periodicity from site to site are shown as the red dots in the figure. The blue dots in the upper range of energies have the same site-to-site periodicity. However, due to the on-site structure the momenta of these wave functions follow more closely the continuation of the low-energy dispersion curve. The continuous curve is drawn using the method presented in Appendix B. We have verified the momentum assignments by evaluating the expectation value of the momentum operator $\partial/i\partial x$. The agreement is approximate but close enough for our purposes.

The amplitudes of the eigenstates on each site can be expressed as

$$(f_{0,m}, f_{1,m}) = e^{im\pi/N_q}(1, \alpha) \quad (13)$$

times an overall factor. Here m labels the site and α controls the mixing of the two states on the site. The mixing amplitude is independent of the site and is purely imaginary for our Hamiltonian. The assigned momentum of this eigenstate is $k = m\pi/(N_q\Delta x)$ or $m\pi/(N_q\Delta x) \pm \pi/N_q$ depending on whether the energy is in the lower or upper half of the spectrum. Note also that right-moving

and left-moving plane waves ψ_k and ψ_{-k} are related by complex conjugation.

Fig. 1 shows the dispersion curve for the ring Hamiltonian with next-to-nearest neighbor interactions and two states on each site. In this calculation, the mesh spacing

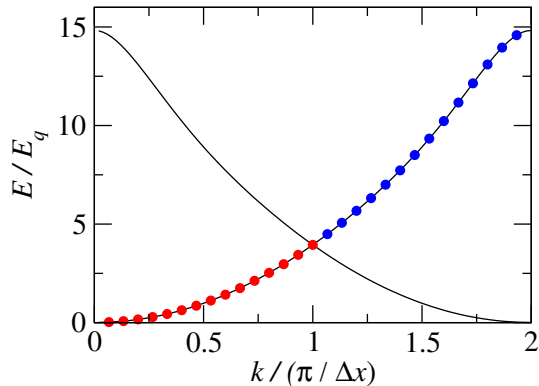


FIG. 1: Energies of plane-wave states in the discrete-basis formalism, as calculated by diagonalizing the ring Hamiltonian with $N_q = 30$ sites. The Hamiltonian and overlap matrices include elements up to second nearest neighbor interactions, $N_{\text{od}} = 2$. Red dots and blue dots show the energies of the lower half and upper half of the eigenenergy spectrum. See text for the assignment of k values to the eigenstates. The lines show the continuous dispersion curve Eqs. (B4,B7-8) derived in Appendix B. See Fig. 2 for comparison with the Schrödinger spectrum.

was set to $\Delta x = 5^{1/2}s$ as in the previous work. Besides diagonal elements, the matrices include off-diagonal elements up to second nearest neighbors. The figure shows that the two-state construction considerably extends the range of momenta that are covered.

Fig. 2 compares the present Hamiltonian to the Schrödinger dispersion curve

$$E = \frac{1}{2M}k^2. \quad (14)$$

The agreement is quite close, and only deviates significantly at the highest momenta. Also shown in the figure are the dispersion curves for the $N_{\text{od}} = 1$ Hamiltonian studied in Ref. [2]. Adding the second state on a site significantly improves the agreement for $|k| < \pi/\Delta x$ as well extending the domain to $k < 2\pi/\Delta x$.

IV. BARRIER PENETRATION IN THE KOHN REACTION THEORY

A. Formalism

The barrier penetration problem may be treated in reaction theory as a system with two active exit channels, namely the transmitted channel on the other side of the

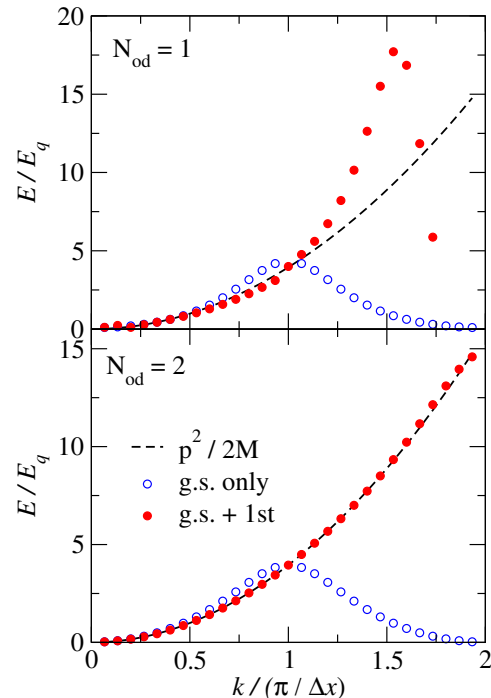


FIG. 2: Energies of plane-wave states in the discrete-basis formalism in the $N_s = 1$ and 2 approximations. The upper and the lower panels show the results with $N_{\text{od}} = 1$ and 2, respectively. The filled red circles show the energies with their Hamiltonian parameters the same as in Fig. 1. Open circles show the energies with $N_s = 1$. The dashed line shows the Schrödinger dispersion curve, Eq. (14).

barrier and the reflected flux within the entrance channel. There are several reaction formalisms based on the S -matrix to treat discrete-basis Hamiltonians. If Hamiltonian in the channel space has the simple form of the one-dimensional nearest-neighbor hopping model, the theory is quite straightforward and it provides numerically exact S -matrix algorithms to calculate reaction observables.

This is not the case when the channel Hamiltonian has a more complex structure. With more than one state on a site, the detailed structure of the channel wave functions has to be included in the boundary conditions on the Hamiltonian. In principle this can be carried out in the S -matrix or the K -matrix formalism, but to deliver numerically exact observables the formalisms require principal-value integrals over states in the interaction regime and channel wave functions. None of our attempts to solve the barrier problem with the wave functions described in our earlier publications were successful. However, we did succeed in getting reasonable results based on Kohn's variational principle [11, 16]. In fact this method has been previously applied to nucleus-nucleus collisions with Hamiltonians constructed by the GCM [17–19] as well as the no-core shell model [14, 20]. The procedure is described below.

The essence of the method is to include at the outset the channel wave functions in the asymptotic region, taking their amplitudes as specific unknown variables to be calculated. In principle it does not matter that the asymptotic channel wave function is wrong in the interaction region because there are other variables in the wave function that will correct them.

In the present problem, there are three channel wave functions to be included, namely: the incoming plane wave ψ_k^L , the reflected plane wave in the same space ψ_{-k}^L , and the outgoing transmitted wave ψ_k^R . There is no incoming wave in the transmitted channel, so it does not appear in the formalism. Each state on a mesh point of the collective coordinate belongs to one of three regions: asymptotic on the left hand side, asymptotic on the right hand side, or in the interacting region in between. The fundamental matrix equation to be solved is Eq. (6) which we now write in the form

$$\mathbf{H}'\psi = (\mathbf{H} - E\mathbf{N})\psi = 0. \quad (15)$$

The goal to solve the equation is approached row by row in the matrix-vector product $\mathbf{H}'\psi$. The full solution will have the form

$$\psi = \psi_k^L + c_1\psi_{-k}^L + c_2\psi_k^R + \sum_{n=1}^{N_\phi/2} \sum_{\mu=0,1} f_{\mu,n}\phi_{\mu,n}. \quad (16)$$

Similar equations to Eqs. (15,16) appear in various forms in many publications using the variational approach to reaction theory. The undetermined amplitudes c_1 and c_2 in Eq.(16) are associated with the channels and the N_ϕ amplitudes $f_{\mu,n}$ are associated with individual GCM states in the interaction region.

To see how Eq. (15) is solved, consider a simplified one having $N_{\text{od}} = 2$ and only a single state on each site. The active elements of the Hamiltonian \mathbf{H}' are depicted in Fig. 3. The top row of the Hamiltonian is zero except for the 5 entries for the kinetic energy operator. It acts on the left hand channel wave function constructed as a linear combination of ψ_k^L and ψ_{-k}^L . Since both wave functions are asymptotic solutions, the row condition $\mathbf{H}'\psi = 0$ is already satisfied. For the next row down, the Hamiltonian may have some contribution from the interaction potential since the kinetic operator extends into the interaction region. Similarly, the next row below extends to two states in that region. The situation is the same on the right hand side of the interaction zone. The lowest row depicted is completely in the asymptotic region, and the Eq. (6) is automatically satisfied by ψ_k^R . The Hamiltonian \mathbf{H}' depicted here also has $N_\phi = 6$ internal states giving the same number of amplitudes $f_1 \dots f_6$ to be determined. Besides those amplitudes for the states in the interaction region, we need to determine the amplitudes c_1 and c_2 for the outgoing channel wave functions. This gives a total $N_\phi + 2 = 8$ unknowns. However there are 10 equations for the 10 rows active in the interaction region, so it appears that the problem is over-determined.

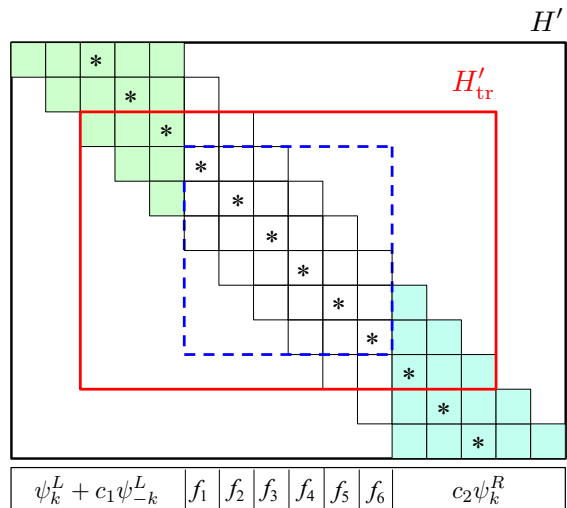


FIG. 3: Active elements of the Hamiltonian for solving the Eq. (15) having parameters $(N_s, N_{\text{od}}) = (1, 1)$. The truncated matrix \mathbf{H}'_{tr} is outlined in red, and the interior elements are encased by the blue dotted square. Active elements in the kinetic part of \mathbf{H}' are indicated by the small boxes. See text for additional details. explanation.

That cannot be a fatal flaw because we know that a solution exists. So there must be a hidden relationship between the amplitudes that allows all 10 row equations to be satisfied. We can find the amplitudes by ignoring two of those rows and solve the algebraic problem of solving 8 equations for 8 linear unknowns. In our implementation, we drop the rows immediately adjacent to the asymptotic region to set up a $(N_\phi + 2) \times (N_\phi + 2)$ matrix to be inverted. In detail, the matrix \mathbf{H}' is truncated to \mathbf{H}'_{tr} with $N_\phi + 2$ rows and $N_\phi + 6$ columns. Then the unknown amplitudes in Eq. (16) are obtained by the matrix inversion of the matrix-vector equation

$$\begin{aligned} & (\mathbf{H}'_{\text{tr}} \cdot \psi_{-k}^L, \mathbf{H}'_{\text{tr}} \cdot \phi_1, \dots, \mathbf{H}'_{\text{tr}} \cdot \phi_{N_\phi}, \mathbf{H}'_{\text{tr}} \cdot \psi_k^R) \begin{pmatrix} c_1 \\ f_1 \\ \vdots \\ f_{N_\phi} \\ c_2 \end{pmatrix} \\ &= -\mathbf{H}'_{\text{tr}} \cdot \psi_k^L \end{aligned} \quad (17)$$

Since the solution of the physical problem is unique, it must be the case that the resulting wave function Eq. (16) also satisfies the condition Eq. (15) for the rows that were dropped. We have checked that that is indeed the case for the numerical examples shown below. Having solved Eq. (17) for the unknown amplitudes, the transmission and reflection probabilities T and R are obtained from the ratio of channel normalizations c_1, c_2 to the incoming wave normalization (equal to one in Eq.

(16)),

$$R = |c_1|^2, \quad T = |c_2|^2. \quad (18)$$

Since there is no absorption of flux, the relation $T+R=1$ should hold.

B. An example

To recapitulate the essential ingredients of the present model, we assume that the GCM states satisfy the Gaussian overlap approximation and construct the \mathbf{H} and \mathbf{N} matrices accordingly. The two parameters controlling the matrix elements of \mathbf{N} are the width of the Gaussian, s in Eq. (2) and the mesh spacing Δx on the collective coordinate. As in our previous studies, distances along the collective coordinate are expressed in units of s and the mesh spacing is taken as $5^{1/2}$ in those units. The kinetic energy operator is the usual one with the unit of energy taken as the zero-point energy of the GCM ground state, Eq. (5). The barrier potential is parameterized as

$$V(x) = V_0 e^{-x^2/2\sigma^2} \quad (19)$$

with V_0 the height of the barrier and σ its width. For this example the width parameter is set to $\sigma = 2.0$. All the needed matrix elements are Gaussian integrals; the formulas are given in the Appendix A. The potential is effective over a region extending to about 10 sites on the chain of GCM states; we take $N_q = 30$ sites and $N_\phi = 60$ basis states in and around the barrier to define the interior region. To define \mathbf{H}'_{tr} the full Hamiltonian is truncated to $N_r = N_\phi + 2$ rows, equal to the number of unknown amplitudes. The number of columns must be $N_\phi + 6$ or larger to accommodate the nonzero Hamiltonian matrix elements in the top and bottom rows. The minimum dimensions of \mathbf{H}'_{tr} are thus 62×66 .

Fig. 4 shows the calculated transmission probability for the above set of Hamiltonian parameters, with a comparison to the direct integration of the Schrödinger equation Eq. (1) and to a previous calculation in the discrete-basis formalism. One sees that present theory is much improved for energies $E/E_q < 3$ and that the catastrophic failure of the previous treatment above that energy is prevented. In the lower panel one sees that the present treatment gives excellent agreement up to at least $E/E_q \approx 10$. That would provide an acceptable energy range to study the role of fission channels in actinide nuclei.

One needs to choose $N_\phi + 2$ rows i from the original Hamiltonian matrix H'_{ij} to define the truncated Hamiltonian, \mathbf{H}'_{tr} . These rows can be arbitrary as long as there is a coupling between the asymptotic wave functions and the internal wave functions. The most appropriate choice would be to take N_ϕ internal rows with 2 extra asymptotic rows on the both sides of a barrier. When there is only one state at each site, this provides a unique choice for \mathbf{H}'_{tr} . On the other hand, when there are two states at

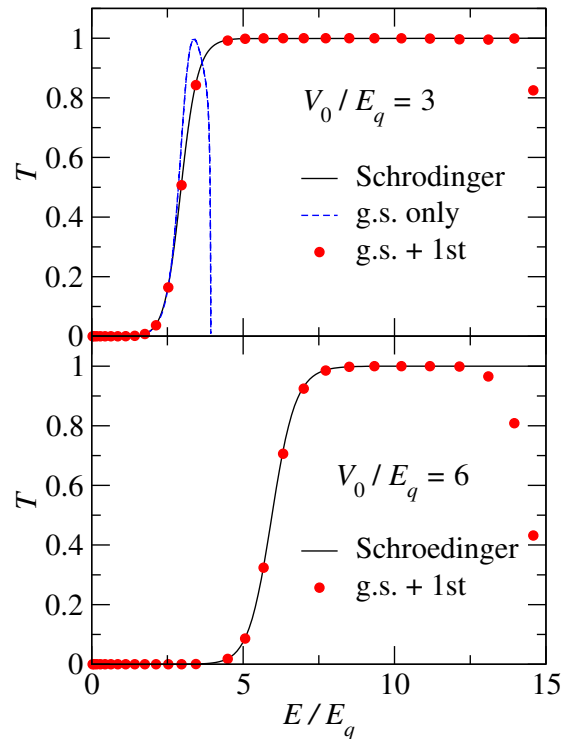


FIG. 4: Transmission probabilities for traversing a barrier computed in the discrete-basis Hamiltonian approximation to the one-dimensional continuum Hamiltonian Eq. (1). The results of the full treatment with $N_s = 2$ and $N_{\text{od}} = 2$ are shown by the red circles. The results from direct integration of the Schrödinger equation are shown by the solid line. The upper panel with barrier height $V_0 = 3E_q$ shows a comparison with the previous published calculation which had only the ϕ_0 states in the basis. In the lower panel the barrier height is $V_0 = 6E_q$, which is beyond the range of the $N_s = 1$ treatment.

each site, there is an ambiguity, as there can be four possible choices, that is, $(\phi_{L,0}, \phi_{R,0})$, $(\phi_{L,0}, \phi_{R,1})$, $(\phi_{L,1}, \phi_{R,0})$, and $(\phi_{L,1}, \phi_{R,1})$ with an obvious notation. We have confirmed that those four choices lead to the same result when N_ϕ is large, such as $N_\phi = 200$. In contrast, when N_ϕ is small, such as $N_\phi = 20$, only the choice $(\phi_{L,0}, \phi_{R,0})$ leads to numerically stable solutions. We found that for the other choices, there is one or two small eigenvalues of the matrix that has to be inverted in Eq. (17). We anticipate that this is the origin of the numerical instability, since all the eigenvalues are large for the choice of $(\phi_{L,0}, \phi_{R,0})$.

V. DISCUSSION

As a study of formalisms for reaction theory, our results extend the range of phenomena that can be studied within the CI approach using the GCM to construct the configurations. Kohn's method gives a general tech-

nique for carrying out numerically accurate calculations of discrete-basis Hamiltonians from a GCM construction. We showed how the formalism can provide reaction branching ratios when there is another exit channel besides the entrance channel.

For nuclear physics and the question about the role of internal channels in fission, the crucial parameters are barrier height and the zero-point energies of the configurations. It appears that these parameters are in a safe region for applying the Kohn formalism and with the present numerical parameters.

However, it should be mentioned that algorithms based on Kohn's treatment are subject to numerical instabilities [21]. This is true for our discrete-basis approach as well. The set of equations Eq. (15,16) is overdetermined, requiring us to ignore some rows in setting up the matrix \mathbf{H}_{tr}^l to be inverted. With a poor choice the matrix is nearly singular and the calculated wave function is not reliable¹. One test for a reliable result is to check flux conservation, i.e., the transmission and reflection probability satisfy $T + R = 1$. We have also found that the method is less sensitive to the choice of rows if the nominal interior space is extended into the channel space.

The computer codes to calculate the $N_s = 2$ data plotted in Fig. 2 and 4 are provided in the Supplementary Material. Also included is a code to compute the plane-wave energy E from Eqs. (B4), (B7), and (B8).

Acknowledgments

This work was supported in part by JSPS KAKENHI Grant Number JP23K03414.

Appendix A: Matrix elements of H, N and V

The Gaussian integrals that arise in calculating the elements of the discrete-basis matrices are evaluated in this appendix. The two physical parameters are s governing the size of the wave packet and E_q , the zero-point energy of the wave packet. The relation to the inertial mass M along the collective coordinate is $E_q = \hbar^2/4Mqs^2$. In the formulas below, lengths are expressed in units of s .

For the overlap matrix N , we write its elements as $\langle \phi_n(x_2) | \phi_{n'}(x_1) \rangle = N_{n,n'}(\Delta x)$ where $\Delta x = x_1 - x_2$. The matrix elements are:

$$N_{00}(\Delta x) = e^{-\Delta x^2/4} \quad (\text{A1})$$

$$N_{01}(\Delta x) = -N_{10}(\Delta x) = -2^{-1/2} \Delta x N_{00}(\Delta x) \quad (\text{A2})$$

$$N_{11}(\Delta x) = (1 - (\Delta x)^2/2) N_{00}(\Delta x) \quad (\text{A3})$$

For the kinetic term T in the Hamiltonian, the matrix elements are

$$T_{00}(\Delta x) = E_q(1 - (\Delta x)^2/2) N_{00}(\Delta x) \quad (\text{A4})$$

$$T_{01}(\Delta x) = E_q(3 - (\Delta x)^2/2) N_{01}(\Delta x) \quad (\text{A5})$$

$$T_{11}(\Delta x) = E_q \left(3 - \frac{3}{2} (\Delta x)^2 \frac{1 - (\Delta x)^2/6}{1 - (\Delta x)^2/2} \right) N_{11}(\Delta x) \quad (\text{A6})$$

Finally the matrix elements of the barrier potential $V(x) = V_0 e^{-x^2/2\sigma^2}$: are:

$$V_{00}(x_1, x_2) = V_0 \sqrt{\frac{2\sigma^2}{2\sigma^2 + 1}} A \quad (\text{A7})$$

$$V_{01}(x_1, x_2) = 2V_0 \frac{-\sigma^2 \Delta x + x_2}{(2 + 1/\sigma^2)^{1/2} (1 + 2\sigma^2)} A \quad (\text{A8})$$

$$V_{11}(x_1, x_2) = 2^{3/2} \sigma V_0 \times \frac{\sigma^4(2 - (\Delta x)^2) + \sigma^2(1 - (\Delta x)^2) + x_1 x_2}{(1 + 2\sigma^2)^{5/2}} A \quad (\text{A9})$$

where A is defined

$$A = \exp \left(-\frac{(1 + \sigma^2)(x_1^2 + x_2^2) - 2\sigma^2 x_1 x_2}{2 + 4\sigma^2} \right). \quad (\text{A10})$$

Eqs. (A7) and (A9) can be conveniently written in factorizable form with the corresponding overlap $N_{n,n'}$ as

$$V_{00}(x_1, x_2) = \tilde{A} N_{00}(\Delta x) \quad (\text{A11})$$

and

$$V_{11}(x_1, x_2) = \left(1 + \frac{1}{1 - (\Delta x)^2/2} \left(\frac{(x_1 + x_2)^2}{2(1 + 2\sigma^2)^2} - \frac{1}{1 + 2\sigma^2} \right) \right) \times \tilde{A} N_{11}(\Delta x), \quad (\text{A12})$$

where

$$\tilde{A} = V_0 \sqrt{\frac{2\sigma^2}{1 + 2\sigma^2}} e^{-\frac{1}{4} \frac{(x_1 + x_2)^2}{1 + 2\sigma^2}}. \quad (\text{A13})$$

The factorizable form for Eq. (A8) is indeterminate at $\Delta x = 0$ because $N_{01}(0) = 0$.

Appendix B: Structure of plane-wave states by the GCM

In this appendix we derive formulas for the energies and structure of GCM continuum wave functions. The application to discrete-basis wave functions is shown at

¹ In Ref. [22], various combinations of rows are tested to maximize the determinant of the matrix.

the end. The total many-body wave function in the multi-channel GCM is given by,

$$\Psi(x) = \sum_i \int dq f_i(q) \psi_{i,q}(x), \quad (\text{B1})$$

where i is a label for the states on a site and q is a generator coordinate. The Hill-Wheeler equation for the weight function $f_i(q)$ reads,

$$\int dq' \sum_{i'} H_{ii'}(q, q') f_{i'}(q') = E \int dq' \sum_{i'} N_{ii'}(q, q') f_{i'}(q'), \quad (\text{B2})$$

with $H_{ii'}(q, q') = \langle \psi_{i,q} | H | \psi_{i',q'} \rangle$ and $N_{ii'}(q, q') = \langle \psi_{i,q} | \psi_{i',q'} \rangle$.

Here we assume translational symmetry requiring the Hamiltonian and the overlap matrices to depend only on the separate of grid points $q - q'$. That is, $H_{ii'}(q, q') = H_{ii'}(0, q' - q)$ and $N_{ii'}(q, q') = N_{ii'}(0, q' - q)$. The solution of the Hill-Wheeler equation, (B2), is then given by,

$$f_i(q) = f_i e^{ikq} \quad (\text{B3})$$

where the energy $E = E(k)$ and the coefficient f_i are determined by solving the generalized eigenvalue problem,

$$\sum_{i'} \tilde{h}_{ii'} f_{i'} = E(k) \sum_{i'} \tilde{n}_{ii'} f_{i'}, \quad (\text{B4})$$

where

$$\tilde{h}_{ii'} = \int dq H_{ii'}(0, q) e^{ikq} \quad (\text{B5})$$

$$\tilde{n}_{ii'} = \int dq N_{ii'}(0, q) e^{ikq}. \quad (\text{B6})$$

The formula corresponding to Eq. (B4) in the discrete-basis formalism is the same with the definitions

$$\tilde{h}_{ii'} = \sum_n H_{ii'}(0, n\Delta x) e^{ink\Delta x} \quad (\text{B7})$$

$$\tilde{n}_{ii'} = \sum_n N_{ii'}(0, n\Delta q) e^{ink\Delta x}. \quad (\text{B8})$$

For the Hamiltonian discussed in the text, $N_s = 2$ states are on a site and Eq. (B4) is the generalized eigenvalue equation with matrices of dimension 2. It can be solved analytically in terms of the elements of the two matrices, but the resulting quadratic equation is not very informative. We note that for discrete-basis Hamiltonian with $N_s = 1$ the Eq. (B4) reduces to the simple form presented in previous publications.

-
- [1] K. Hagino, Phys. Rev. C **109** 034611 (2024).
 - [2] G.F. Bertsch and K. Hagino, Phys. Rev. C **109** 054606 (2024).
 - [3] H.A. Kramers, Physica 7 284 (1940).
 - [4] N.Bohr and J.A. Wheeler, Phys. Rev. 56 426 (1939).
 - [5] P. Bonche, J. Dobaczewski, et al., Nucl. Phys. **A510** 466 (1990).
 - [6] D.L. Hill and J.A. Wheeler, Phys. Rev. **89** 1102 (1953).
 - [7] M. Sin, R. Capote, M.W. Herman, and A. Trkov, Phys. Rev. C **93** 034605 (2016).
 - [8] A.Konig, S. Hillaire and S. Goriely, Eur. Phys. J A **529** 131 (2023).
 - [9] S.A. Bennett et al., Phys. Rev. Lett. **130** 202501 (2023).
 - [10] T. Kawano, P. Talou, and S. Hillaire, Phys. Rev. C **109** 044610 (2024).
 - [11] W. Kohn, Phys. Rev. **74** 1763 (1948).
 - [12] P. Ring and P. Schuck, *The Nuclear Many-Body Problem*, (Springer, Heidelberg), (1980).
 - [13] G.F. Bertsch and W. Younes, Ann. Phys. **403** 68 (2019).
 - [14] V.D. Efros, Phys. Rev. C **99**, 034620 (2019).
 - [15] K. Kravvaris and A. Volya, Phys. Rev. Lett. **119** 062501 (2017).
 - [16] L. Hulthén, Arkiv for Matematik, Astronomi och Fysik, **35A** No. 25 (1948).
 - [17] R. Beck, J. Borysowicz, D.M. Brink and M.V. Hihailović, Nucl. Phys. **A244** 58 (1975).
 - [18] Y. Mito and M. Kamimura, Prog. Theo. Phys. 56 583 (1976).
 - [19] M. Viviani, L. Girlanda, A. Kievsky, and L.E. Marcucci, Phys. Rev. C **102**, 034007 (2020).
 - [20] M.A. Sharaf, A.M. Shirokov, W. Du, and J.P. Vary, arXiv:2408.05656.
 - [21] C.Drischler et al., Phys. Lett. B **823** 136777 (2021).
 - [22] D.Odell, et al., Phys. Rev. C **109** 044612 (2024).